

Artificial Neural Network based fatigue life assessment of riveted joints in AA2024 aluminum alloy plates and optimization of riveted joints parameters

Reza Masoudi Nejad^{1,*}, Nima Sina², Wenchen Ma³, Wei Song⁴, S. P. Zhu⁵, Ricardo Branco⁶, Wojciech Macek⁷, Aboozar Gholami⁸

¹Department of Civil Engineering, School of Human Settlements and Civil Engineering, Xi'an Jiaotong University, Xi'an, China

²Department of Mechanical Engineering, Iowa State University, Ames, IA, USA

³Tesla Inc, 1 Tesla Road, Austin, TX 78725, USA

⁴School of Mechanical & Electrical Engineering, Xuzhou University of Technology, Xuzhou 221018, China

⁵School of Mechanical and Electrical Engineering, University of Electronic Science and Technology of China, Chengdu, 611731, China

⁶University of Coimbra, CEMMPRE, Department of Mechanical Engineering, Coimbra, Portugal

⁷Gdansk University of Technology, Faculty of Mechanical Engineering and Ship Technology, 11/12 Gabriela Narutowicza, Gdańsk 80-233, Poland

⁸Department of Mechanical Engineering, Foolad Institute of Technology, Isfahan, Iran

Abstract

The objective of this paper is to provide the fatigue life of riveted joints in AA2024 aluminum alloy plates and optimization of riveted joints parameters. At first, the fatigue life of the riveted joints in AA2024 aluminum alloy plates is obtained by experimental tests. Then, an artificial neural network is applied to estimate the fatigue life of riveted lap joints based on the number of lateral and longitudinal holes, punch pressure, gap between the edge of hole and rivet, rivet shank diameter, and rivet shank length. Also, meta heuristic optimization algorithm is applied to calculate the riveting process parameters. Finally, sensitivity analysis is used to obtain the influence of parameters affecting the riveting process on the fatigue life.

Keywords: Artificial Neural Network; Structure; Fatigue life; AA2024 aluminum alloy; Riveted lap joint.

1. Introduction

Fatigue failure of riveted lap joints in aircraft joint and bridges building can lead to a major disaster [1-4]. Many researchers used some methods such as fracture mechanics [5], local stress-strain, and local strain energy to predict the fatigue life of the riveted joints in Al-alloy plates, focusing

* Corresponding author.

E-mail addresses: masoudinejad@xjtu.edu.cn (R. Masoudi Nejad), nimasina@iastate.edu (N. Sina), wenchma@tesla.com (W. Ma), swingways@hotmail.com (W. Song), zspeng2007@uestc.edu.cn (S. P. Zhu), ricardo.branco@dem.uc.pt (R. Branco), wojciech.macek@pg.edu.pl (W. Macek).

1
2
3
4 on the effect of riveting process parameters [6]. Ding et al. [7] investigated the relationship
5 between local strain energy density and fatigue life of riveted Al-Li alloy plate. Korbel [8] studied
6 the effect of riveting process parameters on residual stresses, clamping stresses and clamping force
7 in thin sheet riveted joints. Fatigue life prediction for critical members in Al-alloy specimen is
8 essential to its in-service safe operation [9]. Tian et al. [10] investigated the effect of countersunk
9 hole depths (0.65, 0.90, and 1.20 mm) on the fatigue performance of the riveted AA2024-T3 alloy.
10 Skorupa et al. [11] extended a semi-empirical fatigue life prediction model for riveted joints
11 representative of the aircraft fuselage skin connections. They investigated the influence of the
12 interference fit between the rivet and the hole using fatigue test results for Al-alloy. In recent years,
13 single-lap adhesive-riveted hybrid joints have attracted considerable attention in the aerospace
14 structures [12].

15
16 The realm of fatigue life prediction has witnessed a paradigm shift with the introduction of
17 artificial neural networks (ANNs) [13, 14]. The conventional methods of fatigue life prediction,
18 which are often based on analytical or numerical models, have been challenged by the capabilities
19 of ANNs. As delineated by Smith et al. [15], ANNs offer a new vista for addressing the
20 complexities inherent in predicting fatigue life, thereby changing the dimensions of material
21 science and engineering. As Zhang et al. [16] highlighted, traditional methods' limitations in
22 fatigue life prediction must be emphasized. These methods are generally fraught with cumbersome
23 calculations and rely heavily on empirical data, which often restricts their applicability to specific
24 conditions. On the contrary, the computational efficiency of ANNs, as noted by Williams et al.
25 [17], makes them a robust tool for tackling problems often deemed too intricate for traditional
26 computational methods. Furthermore, data-driven approaches in material science are gaining
27 momentum, especially in the context of fatigue life prediction. Thompson et al. [18] have
28 highlighted the growing relevance of data-driven methods, particularly ANNs, in offering more
29 reliable and accurate predictions. These methods can handle a wide range of parameters and
30 conditions, a feature that becomes increasingly relevant when focusing on specific applications
31 such as riveted joints in aerospace structures. Smith et al. [19] have already applied ANNs in
32 estimating the fatigue life of such riveted joints, providing compelling evidence for the reliability
33 of ANN-based models. Integrating ANN with other analytical methods has shown promise in
34 elevating the accuracy and reliability of fatigue life predictions. For instance, Brown et al. [20]
35 have explored the potential of integrating ANN with finite element analysis for assessing the
36
37
38
39
40
41
42
43
44
45
46
47
48
49
50
51

1
2
3
4 fatigue life of marine riveted joints. Such hybrid approaches combine the strength of computational
5 power and pattern recognition, leading to more holistic models. Kim et al. [21] further extended
6 this dialogue by exploring the application of convolutional neural networks (CNNs) in fatigue life
7 prediction, which adds an extra layer of complexity and efficiency. The temporal aspects of
8 fatigue, another crucial parameter, have also been examined through recurrent neural networks
9 (RNNs). Wu et al. [22] provided insights into the applicability of RNNs in capturing these temporal
10 variations, thereby improving predictive models. Sensitivity analysis is another vital area where
11 ANNs have shown considerable promise. As elucidated by Williams et al., [23] sensitivity
12 analysis, when performed on ANN-based models, can provide a more granular understanding of
13 the contributions of each parameter, thereby allowing for more precise engineering designs.
14 Moreover, optimizing materials and processes for enhanced fatigue life is an area where hybrid
15 models have shown potential. Chen et al. [24] discussed the synergies between ANNs and Genetic
16 Algorithms (GA) in material science applications. Patel et al. [25] extended this notion further by
17 incorporating Particle Swarm Optimization with ANN, showing effective results in fatigue life
18 prediction. Despite these advancements, challenges remain. Robinson et al. [26] emphasized
19 standardizing methodologies and addressing the computational constraints often associated with
20 ANN-based predictive models. Their work delineates the roadmap for future research in this
21 domain, advocating for a multi-disciplinary approach to overcome existing challenges.

22
23
24
25
26
27
28
29
30
31
32
33
34
35
36
37
38
39
40
41
42
43
44
45
46
47
48
49
50
51
In order to optimize the effective parameters on fatigue life of riveted joints, first, the precise
understanding of the process and its effective parameters have been discussed. The effect of
parameters is examined and the desired output is obtained. Also, the fatigue life of the riveted
joints is obtained by experimental tests. Then an ANN is used to calculate the fatigue life of riveted
lap joints in AA2024 aluminum alloy plates, taking a step towards understanding its longevity
based on the six parameters. Also, meta heuristic optimization algorithm is applied to predict the
best riveting process parameters.

2. Materials and methods

One of the basic engineering requirements in design was the need to understand the different ways
in which materials or parts were exhausted. Exhaustion is usually associated with fatigue failure
or large deformation. This fatigue failure is well known under static, tensile, compressive and shear
loads. Mechanical exhaustion causes many injuries and costs. However, due to the proper design

of the components and engineering structures, these exhaustions have been reduced to the least amount. The objective of this study is to study the fatigue life of the riveted joints in AA2024 aluminum alloy plates. Plates and rivets are built from AA2024 aluminum alloy (Fig. 1). The mechanical properties of the materials are presented in Table 1 [2]. Also, effective parameters on the fatigue life of the riveted lap joints are presented in Table 2. The effective parameters on fatigue life of riveted joints are presented in Table 3 and subsequently the fatigue life of the riveted joints in AA2024 aluminum alloy plates is achieved by laboratory tests. Fig. 2 shows the geometry of riveted lap joint [1].

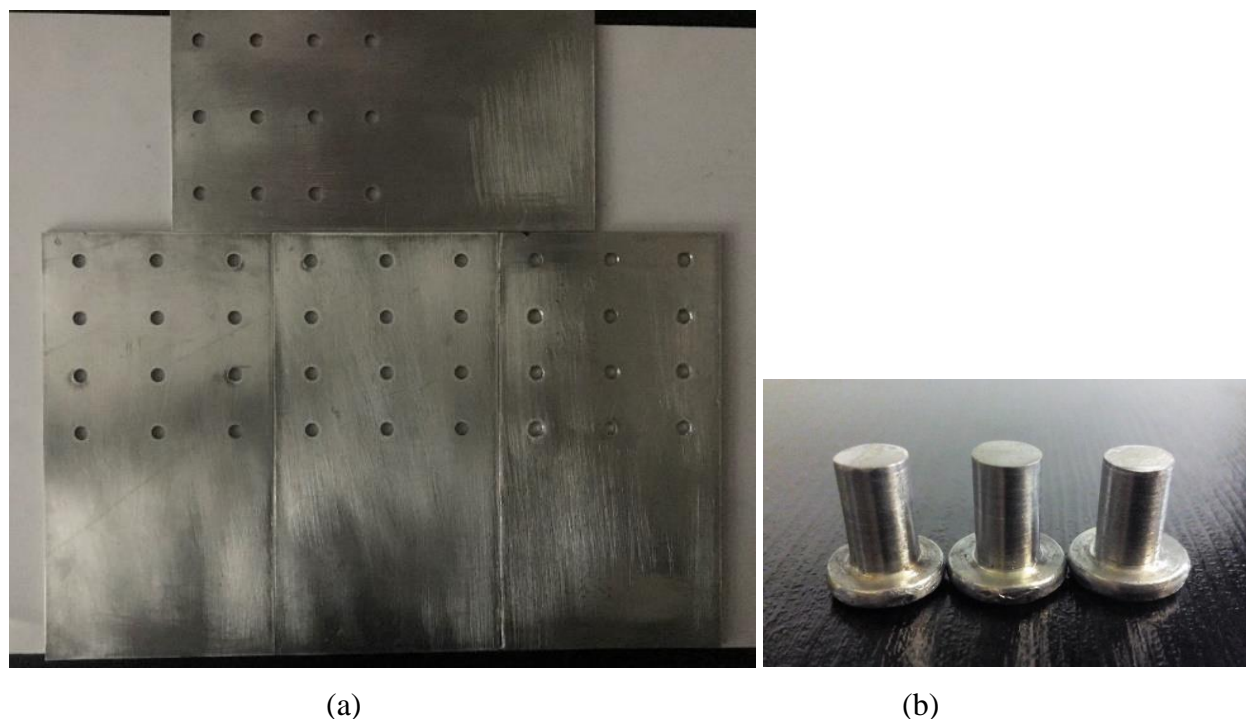


Fig. 1. Plates and rivets used for experimental tests. a) Al2024-T3 plates, b) Al2024-T3 rivets.

Table 1. Mechanical properties of materials used in laboratory tests [1].

Related model	material	Young modulus [MPa]	Poisson ratio	Yield strength [MPa]	Ultimate tensile strength [MPa]
rivet	Al2024-T4	69824.3	0.33	244.38	402.63
plate	Al2024-T3	71572.0	0.33	378.02	571.92

Table 2. The effective parameters on fatigue life of riveted joints [1].

parameters	Symbol	Level 1	Level 2	Level 3	Level 4
Rivet shank length	h [mm]	6	7	8	9
Rivet shank diameter	d [mm]	2.8	3.8	4.8	5.8
Gap between the edge of hole and rivet	gap [mm]	0	0.2	0.4	0.6
Punch pressure	P [MPa]	1.2Sy	1.4Sy	1.6Sy	1.8Sy
the number of lateral holes	n_lat	1	2	3	4
the number of longitudinal holes	n_long	1	2	3	4

Table 3. The specimen configuration of riveted joints for experimental tests.

Specimen No.	Parameter 1	Parameter 2	Parameter 3	Parameter 4	Parameter 5	Parameter 6
LP-AI-01	6	2.8	0	1.2*Sy	1	1
LP-AI-02	6	3.8	0.2	1.4*Sy	2	2
LP-AI-03	6	4.8	0.4	1.6*Sy	3	3
LP-AI-04	6	5.8	0.6	1.8*Sy	4	4
LP-AI-05	7	2.8	0	1.4*Sy	2	3
LP-AI-06	7	3.8	0.2	1.2*Sy	1	4
LP-AI-07	7	4.8	0.4	1.8*Sy	4	1
LP-AI-08	7	5.8	0.6	1.6*Sy	3	2
LP-AI-09	8	2.8	0.2	1.6*Sy	4	1
LP-AI-10	8	3.8	0	1.8*Sy	3	2
LP-AI-11	8	4.8	0.6	1.2*Sy	2	3
LP-AI-12	8	5.8	0.4	1.4*Sy	1	4

LP-AI-13	9	2.8	0.2	1.8*Sy	3	3
LP-AI-14	9	3.8	0	1.6*Sy	4	4
LP-AI-15	9	4.8	0.6	1.4*Sy	1	1
LP-AI-16	9	5.8	0.4	1.2*Sy	2	2

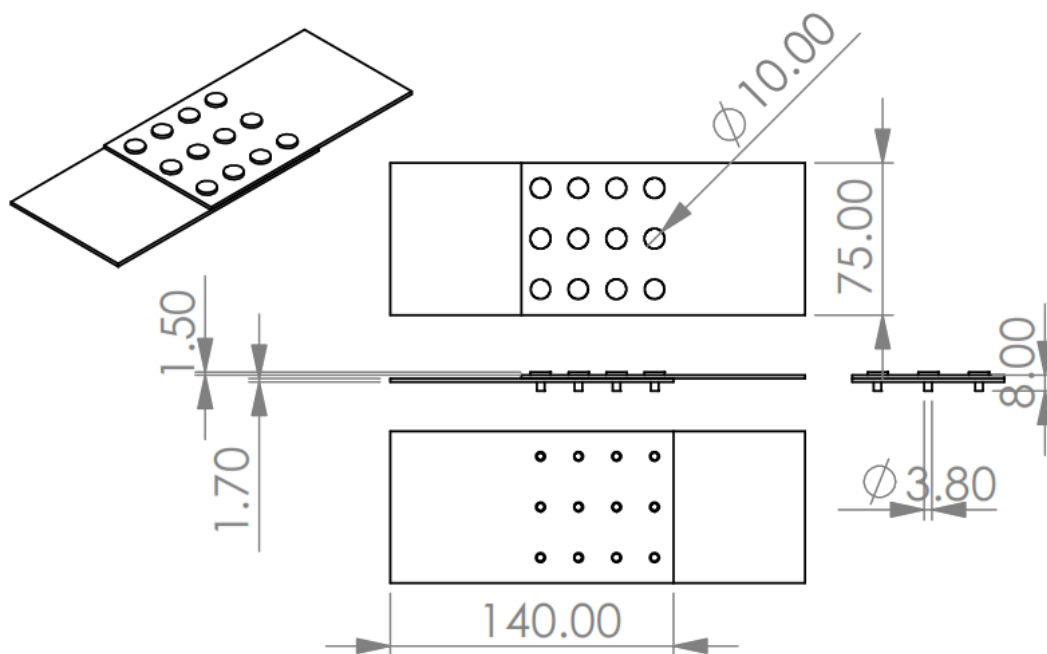


Fig. 2. Geometry of riveted joints used in laboratory tests (dimensions in mm) [1].

However, by considering the correct design in engineering structures, the fatigue failure has been minimized. But the cost of these failures is very high. There are many methods to design based on concepts of fatigue. These methods can be simple and inexpensive or very complicated and expensive. In this paper, the fatigue life of the specimens is achieved by the Zwick machine in force-control mode with a maximum force of 23 kN and $R=0.1$. A frequency of 10 Hz is selected for laboratory tests. Fig. 3 shows the experimental test setup. The test steps, such as installing the riveted joint on the machine, applying cyclic loading and finally joint fracture step are defined according to [1]. Also, the specimens presented in Table 3 are applied under fatigue loading with the same conditions.



Fig. 3. Experimental test setup for fatigue life estimation.

3. The Structure and Applications of ANNs

3.1. ANN Architecture

The development trajectory of ANNs provides a compelling narrative of incremental advances and paradigm shifts within the computational sciences. Early theoretical foundations were laid by work that drew inspiration from biological neural systems, offering seminal insights into the logical calculus of neural activities [27]. This work was further expanded upon through psychological and computational models that explored learning and memory mechanisms akin to neurobiological processes [18]. As computational power grew during the latter part of the 20th century, the practical feasibility of employing ANNs for problem-solving became apparent. Breakthroughs in training algorithms, most notably the Backpropagation algorithm, were pivotal in this evolution [29]. Further progress was facilitated by advances in algorithmic paradigms and architectural designs [30], which heightened the networks' capability to model complex, nonlinear systems with remarkable fidelity. These capabilities have not only broadened the applicability of ANNs across diverse scientific and industrial sectors but have also cemented their role as a cornerstone in computational modeling techniques [31]. In contemporary settings, ANNs are routinely employed for a myriad of applications, from predictive analytics and data mining to control systems and operations research. These networks, particularly effective at forecasting outcomes of intricate systems even with inherent nonlinearities, have firmly established themselves as one of the most

important computational tools. ANNs are inspired by the architecture of the human brain's biological neural systems. Artificial neurons are the processing units in the concept of ANN's. Each artificial neuron takes an input signal, undergoes a series of mathematical computations, and produces an output. Mathematically, this is represented in Eq. (1).

$$y = \varphi \left(b + \sum_{i=1}^m x_i w_i \right) \quad (1)$$

where x_i is represents input values, w_i is indicates weights, m is stands for the total number of data samples, b is the bias, and φ is symbolizes the activation function.

The general architecture of an ANN encompasses three distinct layers: input, hidden, and output. For this study, a feed-forward ANN has been employed. A feed-forward ANN is a type of ANN where connections between nodes (neurons) do not form any cycles, meaning data flows in one direction, from input to output. The network typically consists of multiple layers, including input, hidden, and output layers, with neurons processing data and transmitting information sequentially through each layer. The primary objective of the ANN is to accurately forecast the fatigue life derived from the inputs for rivet material. The input parameters are considered as $X = \{x_1, x_2, x_3, x_4, x_5, x_6\}$. These parameters are defined in Table 4.

Table 4. The input parameters for ANN.

Input Parameters	Name
x_1	Rivet shank length
x_2	Rivet shank diameter
x_3	Gap between the edge of hole and rivet
x_4	Punch pressure
x_5	The number of lateral holes
x_6	The number of longitudinal holes

1
2
3
4 Given the single predictive parameter, only one neuron is necessary for the output layer. The
5 training data helps calibrate the neuron's weights and biases. In contrast, the validation set refines
6 the training process, and the testing data measures the overall efficacy post-learning. Data points
7 for this study have been segmented into two subsets: Specifically, 70% of the entire data serves
8 the training phase, 30% is allocated for testing. A noteworthy aspect of proficient ANNs is the
9 absence of overfitting. Overfitting arises when an ANN, despite being adept at predicting training
10 data, fails to maintain the same accuracy with the test dataset. Factors influencing the ANN's output
11 include the number of neurons in the hidden layer, the type of activation function, and the chosen
12 learning algorithm. Here, the activation function employed is a tangent sigmoid function, detailed
13 further in Eq. (2).
14
15
16
17
18
19
20
21

$$\tan sig(n) = \frac{1}{1 - e^{-2n}} - 1 \quad (2)$$

22
23
24
25
26 Widely used in ANN learning, the algorithm tests various neuron numbers in the hidden layer to
27 determine optimal performance, detailed in Eq. (3).
28
29

$$MSE = \frac{1}{n} \sum_{i=1}^n (Y_i - \hat{Y}_i)^2$$

30
31
32
33 (3)

34
35
36 Y_i represents the experimental value and \hat{Y}_i the ANN output, with n as the total data points. The
37 method to identify the ideal neuron number is illustrated in Fig. 4.
38

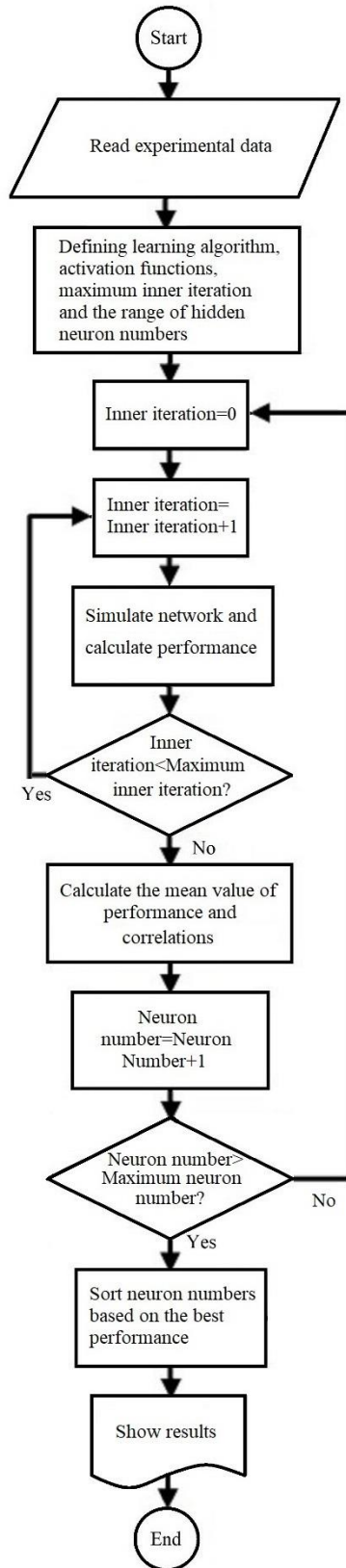


Fig. 4. The flow chart of algorithm for obtaining the optimum neuron number [13].

3.2. Optimization

Optimization seeks the best problem solution, either to minimize or maximize. Multi-objective optimization is presented in Eq. (4).

$$\min(f(\vec{x})), \vec{x} \in X \quad (4)$$

In which X denotes the decision vector and f is the cost function. The GA, a renowned metaheuristic inspired by natural selection, offers benefits over traditional algorithms. It utilizes mutation, crossover, and selection operations, emphasizing iterative evolution to better solutions. With every cycle, possible solutions are evaluated, and those with superior results become the succeeding generation's parents. The crossover, mutation, and combination with parent genes lead to selection of top solutions, with termination usually upon reaching a predetermined generation count or if optimal results plateau. GA's crossover operation ensures diverse solutions by blending parent genes.

After gene blending, top solutions are chosen, often via the stochastic roulette wheel method, wherein selection probability is based on solution efficacy. Thus, optimal solutions gain larger segments. As the total population comprises n entities, probability summation is one, necessitating cost function normalization between zero and one. In analyzing a population size of n individuals, the consequent probability acquired can be delineated by Eq. (5).

$$P_x = \frac{f_x}{\sum_{i=1}^n f_i} \quad (5)$$

Drawing a parallel with the Roulette wheel mechanism, it becomes evident that the most optimal solutions tend to occupy larger segments, thereby increasing their likelihood of being selected. A comprehensive illustration of the GA is depicted in Fig. 5.

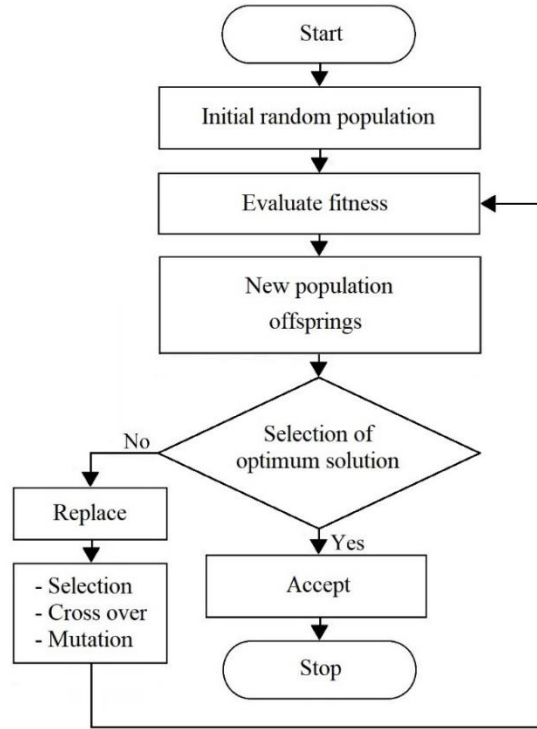


Fig. 5. A comprehensive illustration of the GA.

4. Results and discussion

4.1. ANN results

In this study, the input parameters of ANN are the number of lateral holes, the number of longitudinal holes, punch pressure, gap between the edge of hole and rivet, rivet shank diameter, and rivet shank length. Also, the target is the fatigue life of riveted lap joints. The experimental test results are presented in Table 5. Also, the optimum network results are presented in Table 6.

Table 5. The experimental test results for riveted lap joints.

Specimen No.	Specimen life [cycles]	Specimen No.	Specimen life [cycles]
LP-AI-01	4211	LP-AI-09	5036
LP-AI-02	4729	LP-AI-10	5156
LP-AI-03	4912	LP-AI-11	6281
LP-AI-04	5497	LP-AI-12	5504

LP-AI-05	4821	LP-AI-13	5767
LP-AI-06	6357	LP-AI-14	5832
LP-AI-07	4469	LP-AI-15	5312
LP-AI-08	5251	LP-AI-16	5914

Table 6. ANN results for fatigue life of riveted lap joints.

Experimental Value	Train results	Test results	Experimental Value	Train results	Test results
4211	4211	-	5036	5036	-
4729	4729	-	5156	-	5030.02
4912	4912	-	6281	6281	-
5497	-	5557.26	5504	5504	-
4821	4821	-	5767	5767	-
6357	-	6094.59	5832	5832	-
4469	-	4399.65	5312	-	5129.96
5251	5251	-	5914	5914	-

The accuracy of ANN results is calculated using the Pearson correlation coefficient, denoted in Eq. (6), where a coefficient nearing one indicates a direct relationship between experimental data and ANN outputs.

$$r = \frac{\sum_{i=1}^n (x_i - \bar{x})(y_i - \bar{y})}{\sqrt{\sum_{i=1}^n (x_i - \bar{x})^2 \sum_{i=1}^n (y_i - \bar{y})^2}} \quad (6)$$

where x is the target, and y is the ANN's output. Also, \bar{x} and \bar{y} are the means of these two values. The performances and Pearson correlation coefficients are presented in Table 7. It should be noted that the results are sorted based on the best performance.

Table 7. The Performances and Pearson correlation coefficient.

Neuron Number	Performance	Correlation Coefficient
12	1.50396E-25	0.990832141
15	2.25595E-25	0.983764285
16	2.25595E-25	0.955752928
19	4.51189E-25	0.949084267
14	2.25595E-25	0.948468488
11	1.99629E-21	0.95236525
17	1.50396E-25	0.933035274
13	2.25595E-25	0.945770466
18	1.21069E-23	0.872405309
10	2.25595E-25	0.917304329
20	3.00793E-25	0.880483057

4.2. The Fitting Method

In the domain of data analytics, fitting methods serve as essential tools. They help data scientists and analysts develop mathematical models that closely align with real-world datasets, even when the data spans multiple dimensions, like this 6-D input data. It's akin to weaving a cohesive story from various data threads. The toolkit for these methods is extensive. Linear and polynomial regressions, for instance, are foundational, offering insights by tracing straight lines or curves through data points. The true power of fitting methods lies in their predictive capabilities. Beyond simply mapping out existing data, they can forecast future trends or outcomes. Once a model is fine-tuned, it becomes an invaluable asset, shedding light on hidden patterns and providing a robust foundation for making informed decisions. In a nutshell, employing fitting methods in data analysis facilitates a more profound understanding of data's intricacies, enabling scientists to craft

strategies and solutions in tangible insights. In this work, using 6-D input parameters fatigue life is predicted. A formula for prediction of fatigue life is presented as follow:

$$y = a_0 + \sum_{i=1}^6 a_i x_i + \sum_{i=1}^6 b_i x_i^2 + \sum_{i=1}^6 \sum_{j=i+1}^6 c_{ij} x_i x_j \quad (7)$$

The first summation captures the linear relationship with each feature. The second summation captures the relationship of each feature squared. The final double summation captures the interaction terms between different features. The actual values for a_i , b_i and c_{ij} coefficients would be determined by the ridge regression model fitting process on the data. The coefficients are shown in Table 8. As the dimension of the input space is 6, it is not possible to depict all dimension in one figure.

The fitting results are presented in Table 9. The absolute value of error for both ANN and fitting method are presented in Fig. 6. It can be seen that the fitting method has better results. Also, the fitting method has smaller errors and can predict the fatigue life accurately.

Table 8. The coefficients of the fitted surface.

Coefficient	a0	a1	a2	a3	a4	a5	a6
Value	5271.859	187.1952	138.5928	138.5928	-426.3669	-13.2432	182.2626
Coefficient	b1	b2	b3	b4	b5	b6	
Value	-125.848	-19.9462	-19.9462	182.482	7.827803	7.827803	
Coefficient	c1	c2	c3	c4	c5	c6	c7
Value	-209.575	-209.575	15.67009	319.5047	-259.952	-19.9462	-65.4786
Coefficient	c8	c9	c10	c11	c12	c13	c14
Value	-23.4579	-30.1517	-65.4786	-23.4579	-30.1517	57.78261	5.480872
Coefficient	c15						

Value 58.94396

Table 9. The actual data and the fitted results.

Data Number	Actual Data	Fitting results	Data Number	Actual Data	Fitting results
1	4211	4211	9	5036	5036
2	4729	4729	10	5156	5030.0257
3	4912	4912	11	6281	6281
4	5497	5557.2687	12	5504	5504
5	4821	4821	13	5767	5767
6	6357	6094.5941	14	5832	5832
7	4469	4399.6513	15	5312	5129.9633
8	5251	5251	16	5914	5914

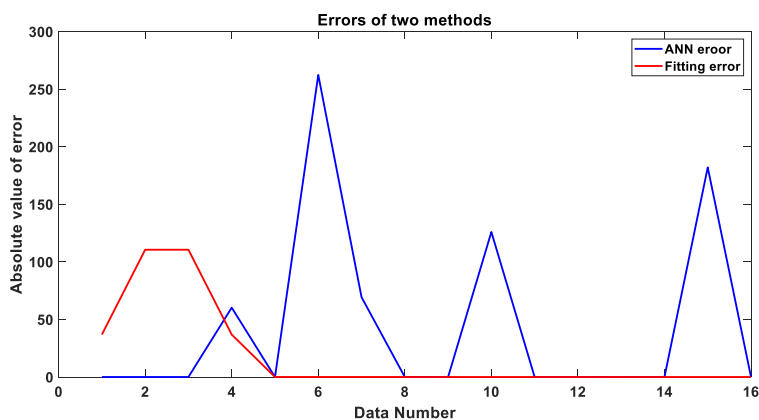


Fig. 6. The absolute value of errors of ANN and fitting method.

4.3. Pairwise 3D Plots for Multi-dimensional Data Visualization

When dealing with datasets with many features, directly holistically visualizing the entire dataset becomes challenging. In the context of this study, for analyzing the impact of six different input features on the fatigue life prediction, a pragmatic and insightful approach is the use of Pairwise 3D Plots. Pairwise 3D plotting entails systematically selecting pairs of features from set and plotting them against the output in a three-dimensional space. By employing this method, a collection of 3D plots is presented, where each one visualizes the interplay between two distinct

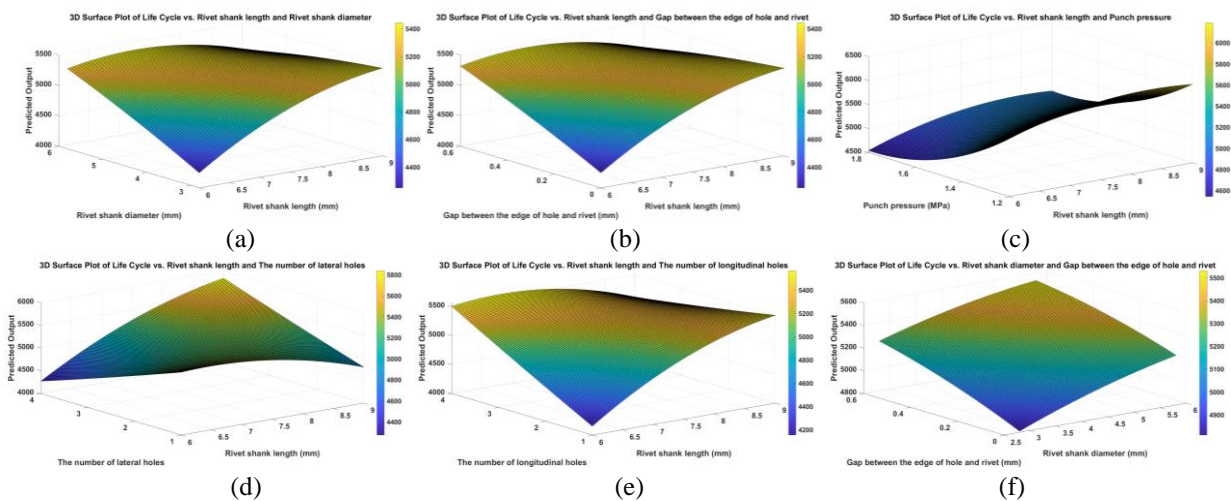
1
2
3
4
5
6
7
8
9
10
11
12
13
14
15
16
17
18
19
20
21
22
23
24
25
26
27
28
29
30
31
32
33
34
35
36
37
38
39
40
41
42
43
44
45
46
47
48
49
50
51
Downloaded from mostwiedzy.pl
MOST WIEDZY

input features and the fatigue life output. Such a pairwise representation allows insights into the interactions and dependencies between individual feature pairs and the predicted output. For example, by juxtaposing rivet shank diameter and rivet shank length in a 3D plot with the fatigue life as the response variable, it is discerned how these two features, in conjunction, influence the fatigue life prediction. By systematically repeating this for all feature combinations, a granular understanding of bivariate interactions across the entire feature set is obtained. This method has some limitations. The visualization simplifies the multivariate relationship. The surface might look different if some other features were changed from its mean. Also, the surface helps understand the role of two features, but it doesn't mean the model can accurately predict the output using only these two features. Removing other features or their interactions from the model would likely affect its prediction accuracy. But in general, this method, while not capturing the entirety of the multi-dimensional interactions in one view, offers a granular perspective, making it easier to pinpoint specific interactions and derive actionable insights. Even though only two features vary in each plot, the model includes interaction terms that may involve other features. These interaction terms remain at values corresponding to the mean values of the non-visualized features.

The equation of the fitted surface based on the features i, j is presented as Eq. (8).

$$y = S_1x_i + S_2x_j + S_3x_i^2 + S_4x_j^2 + S_5x_ix_j + S_6 \quad (8)$$

So, while the visualization focuses on two primary features, the underlying model still incorporates information from all features in these interactions. These features are depicted in Fig. 7.



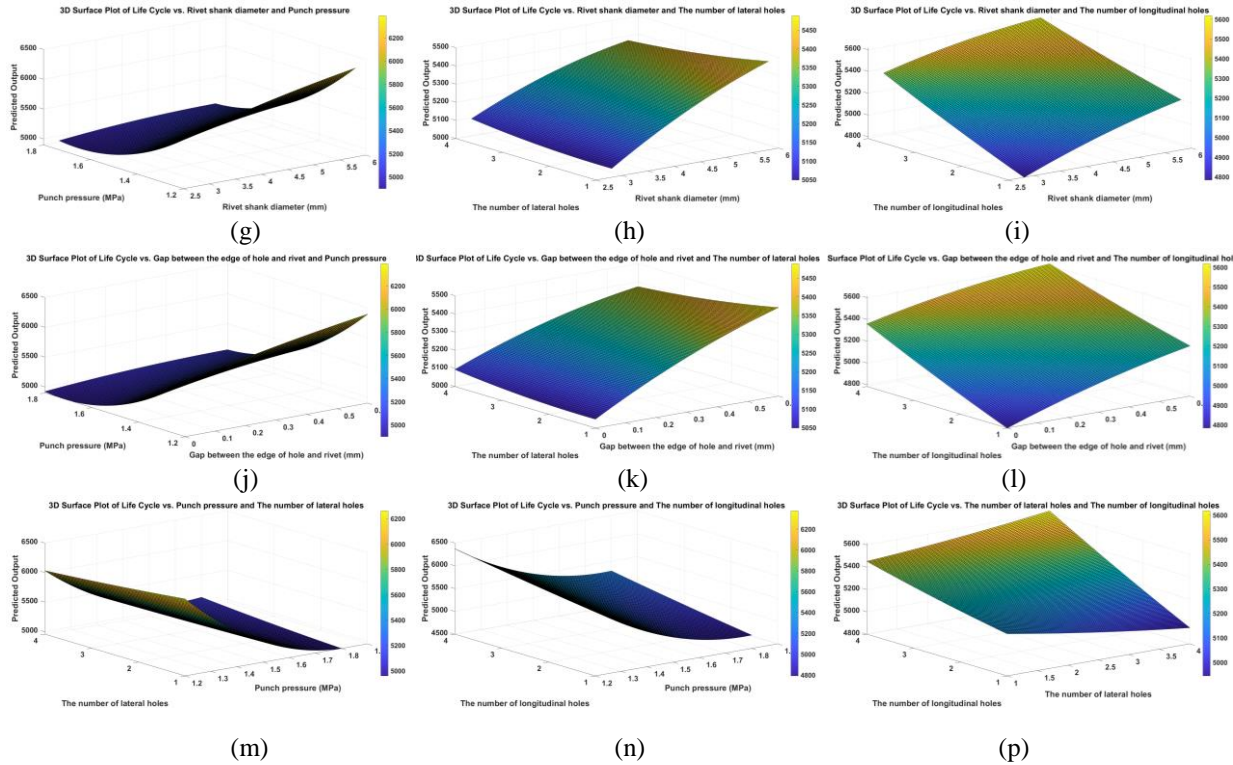


Fig. 7. The surface of fatigue life of riveted lap joints vs.; a) x_1 and x_2 , b) x_1 and x_3 , c) x_1 and x_4 , d) x_1 and x_5 , e) x_1 and x_6 , f) x_2 and x_3 , g) x_2 and x_4 , h) x_2 and x_5 , i) x_2 and x_6 , j) x_3 and x_4 , k) x_3 and x_5 , l) x_3 and x_6 , m) x_4 and x_5 , n) x_4 and x_6 , p) x_5 and x_6 .

As shown in Fig. 7, the combined effects of two features on the output are visualized. In these figures, each 3D surface plot provides a snapshot of how the output changes as two particular features vary while all other features are held at their mean values. The coefficients of the fitted surfaces of Fig. 7 are presented in Table 10.

Table 10. The coefficients of the fitted surfaces.

Surface Number	S1	S2	S3	S4	S5	S6
1	187.2	138.59	-125.85	-19.95	-209.58	5271.86
2	187.2	138.59	-125.85	-19.95	-209.58	5271.86
3	187.2	-426.37	-125.85	182.48	15.67	5271.86
4	187.2	-13.24	-125.85	7.83	319.5	5271.86
5	187.2	182.26	-125.85	7.83	-259.95	5271.86
6	138.59	138.59	-19.95	-19.95	-209.58	5271.86

7	138.59	-426.37	-19.95	182.48	15.67	5271.86
8	138.59	-13.24	-19.95	7.83	319.5	5271.86
9	138.59	182.26	-19.95	7.83	319.5	5271.86
10	138.59	-426.37	-19.95	182.48	319.5	5271.86
11	138.59	-13.24	-19.95	7.83	-259.95	5271.86
12	138.59	182.26	-19.95	7.83	-19.95	5271.86
13	-426.37	-13.24	182.48	7.83	-65.48	5271.86
14	-426.37	182.26	182.48	7.83	-23.46	5271.86
15	-13.24	182.26	7.83	7.83	-23.46	5271.86

4.4. Optimization Results

One of the goals of this paper is to obtain optimum values for input parameters to maximize the fatigue life. The range of six input parameters are defined in Table 11. Also, the GA settings are presented in Table 12.

Table 11. The range of input parameters.

Value	x1	x2	x3	x4	x5	x6
Min	6	2.8	0	1.2	1	1
Max	9	5.8	0.6	1.8	4	4

Table 12. The GA settings.

Maximum number of iterations	Number of populations	Crossover percentage	Mutation Percentage	Mutation rate
30	50	0.8	0.3	0.02

GA tries different values for the input parameters and it should be able to know the value of the target function. Here, target function is defined as the fatigue life. As there is not a specific target function based on the input values, it is impossible to evaluate the value of target by experiments and that's why the obtained fitting function is used for this purpose. Therefore, the GA and the fitting function are connected and have interactions and can find the optimum design vector which

leads to the maximum number of fatigue life. The history of target function based on the number of function evaluation (NFE) is depicted in Fig. 8. It can be seen that after a while, there is no improvement in the target function. Also, the optimum results of GA are presented in Table 13.

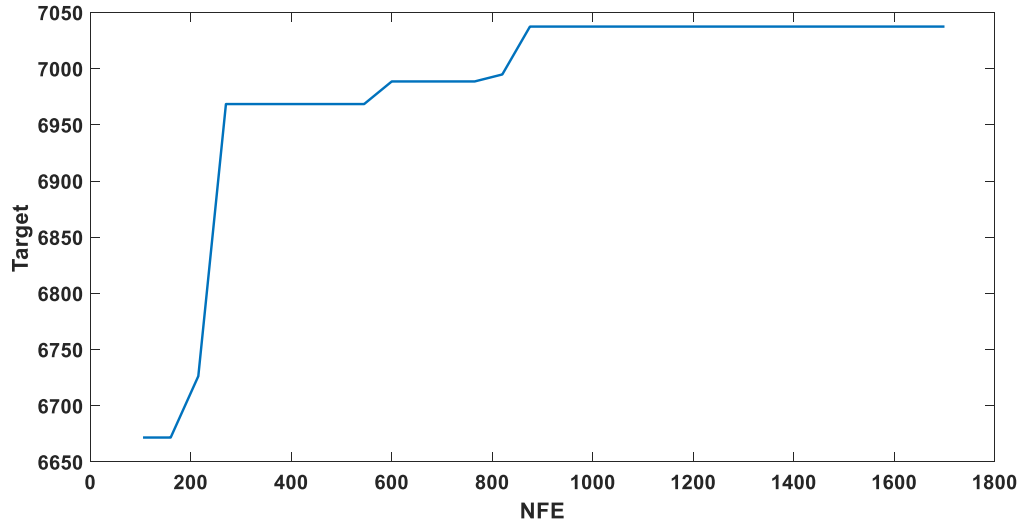


Fig. 8. The history of target function based on the NFE.

Table 13. The optimum values of design vector.

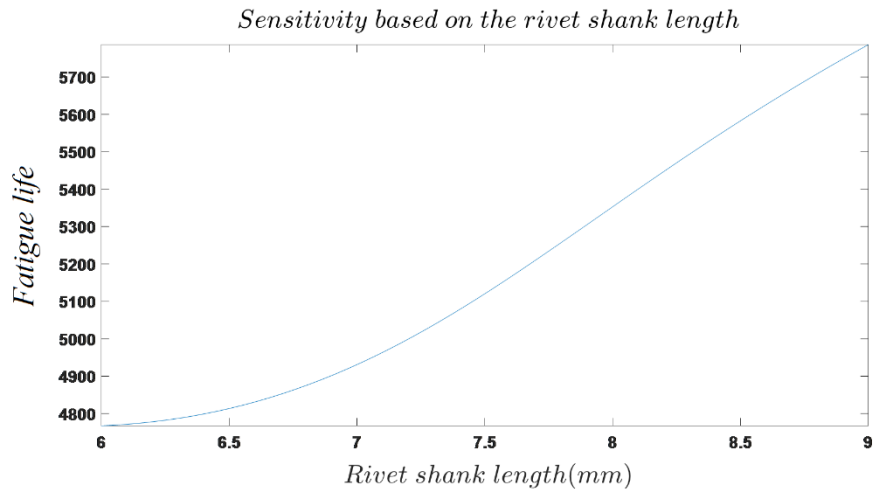
Name	x1	x2	x3	x4	x5	x6
Value	8	3.5	0.6	1.2	4	4

4.5. Sensitivity analysis

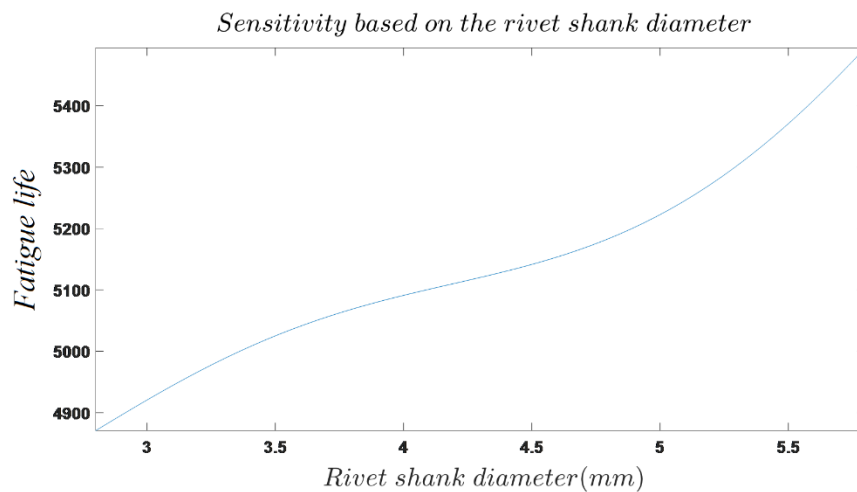
In engineering, sensitivity analysis helps understand the robustness and reliability of system designs by assessing how parameter variations affect system performance. This can be crucial for optimizing designs, identifying potential weak points, and ensuring safety and reliability. Applications include structural design optimization, system reliability assessment, and understanding uncertainties in simulation models. The decisions about design improvements and risk management through sensitivity analysis can be understood.

Another aspect of this research involves executing a sensitivity analysis on the ANN, aiming to elucidate the influence of varying input magnitudes on fatigue life. For ascertaining the ANN's sensitivity, if there are n input parameters, $n-1$ parameters remain static at their average value, the remaining parameter is allowed to fluctuate within its bounds. This procedure is reiterated for all six input variables, with subsequent calculation of fatigue life. The sensitivity figures are shown

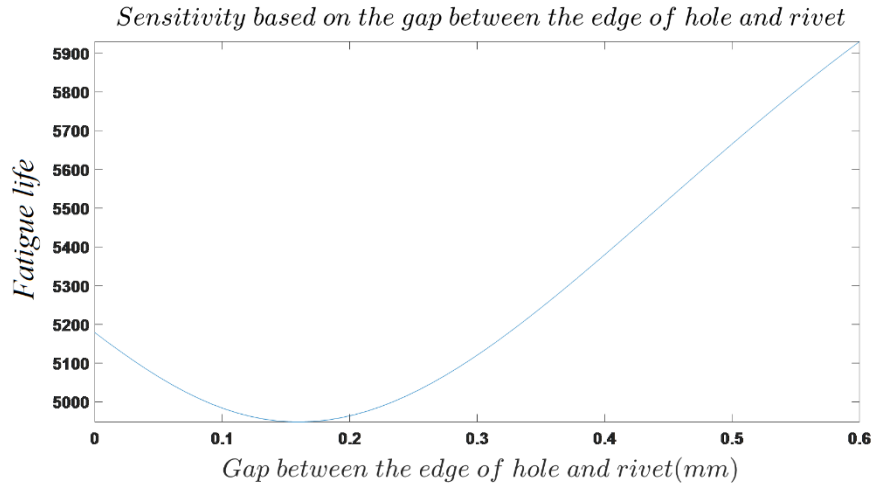
in Fig. 9. As shown in Fig. 9-a, it can be seen that as the rivet shank is increased, the fatigue life will be increased too. Therefore, there is a direct relationship between these two. According to Fig. 9-b, the fatigue life has a direct relationship with rivet shank diameter. According to Fig. 9-c, the minimum fatigue life happens when the gap between the edge of hole and rivet is 0.15 mm and the maximum fatigue life is at 0.6 mm. The minimum fatigue life happens when the punch pressure is increased (Fig. 9-d). In other words, the fatigue life and punch pressure have a reverse relationship. It is seen in Fig. 9-e that the minimum fatigue life happens when the number of lateral holes is three and to reach the maximum fatigue life, the number of lateral holes should be minimum which is 1. It is seen in Fig. 9-f that the minimum fatigue life happens when the number of longitudinal holes is increased. The fatigue life and the number of longitudinal holes have a direct relationship.



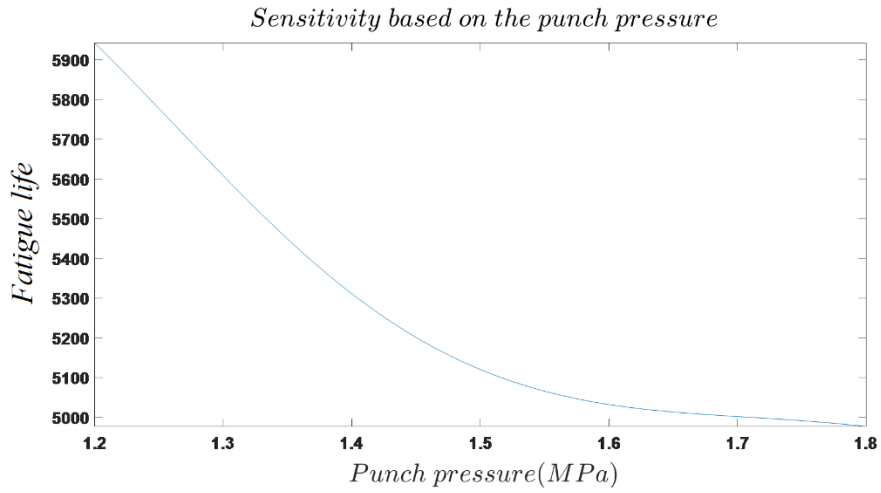
(a)



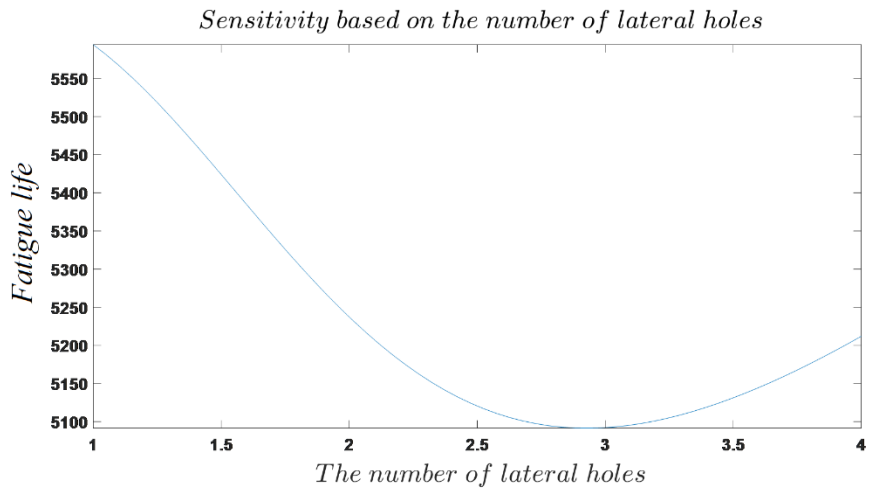
(b)



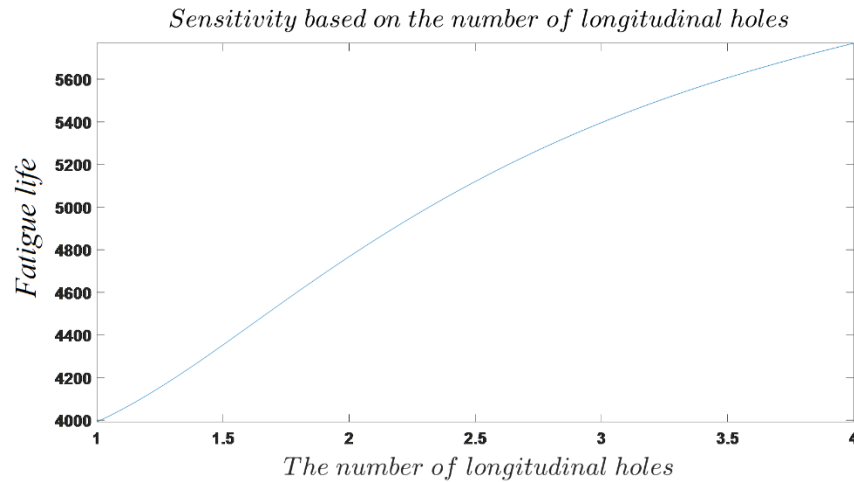
(c)



(d)



(e)



(f)

Fig. 9. The sensitivity analysis for; a) the rivet shank length, b) the rivet shank diameter, c) the gap between the edge of hole and rivet, d) the punch pressure, e) the number of lateral holes, f) the number of longitudinal holes.

5. Conclusions

In this paper, the fatigue life of riveted lap joints was effectively predicted through the utilization of an artificial neural network. Consistency and reliability in predictions were observed, thereby validating the role of ANNs as robust tools for interpreting the effects of multiple parameters on material fatigue life. A noteworthy advancement was achieved through the integration of the ANN with a GA. In this setting, the predictive capability of the ANN was employed as a target function for the GA, leading to the identification of optimal solutions within the parameter space. This collaborative approach between ANN and GA is posited to introduce a novel paradigm with potential applications extending beyond material science into broader engineering disciplines. Significant insights were gained through a comprehensive sensitivity analysis, which was executed to understand how individual parameters influence the fatigue life of riveted joints. It was revealed that the rivet shank length and diameter have a direct relationship with increased fatigue life. On the other hand, an inverse relationship was observed for parameters such as punch pressure and the number of lateral holes. In particular, the sensitivity analysis demonstrated the criticality of optimizing the gap between the edge of the hole and the rivet, as well as punch pressure, to enhance fatigue life. Moreover, the role of each parameter in fatigue life prediction was meticulously examined. For instance, while parameters like rivet shank length and diameter were shown to be

1
2
3
4 directly proportional to increased fatigue life, parameters such as punch pressure exhibited a
5 negative influence, highlighting the need for focused design interventions in these areas.
6
7 Conclusively, the study furnishes a methodical approach that synergizes computational
8 intelligence with experimental analyses. This approach not only allows for enhanced fatigue life
9 prediction but also provides actionable insights for design optimization. Recommendations for
10 future work include refining the ANN model and extending the methodology to additional material
11 combinations and loading conditions, aiming to further validate the robustness and applicability
12 of this integrated approach.
13
14
15
16
17
18

19 **Acknowledgment**

20
21 This study is financially supported by the Top Young Talent Programme of Xi'an Jiaotong
22 University (Project No. 011900/71211223030701).
23
24
25

26 **References**

- 27
28 [1] Reza Masoudi Nejad, Mohammadreza Tohidi, Ahmad Jalayerian Darbandi, Amin Saber,
29 Mahmoud Shariati. Experimental and numerical investigation of fatigue crack growth behavior
30 and optimizing fatigue life of riveted joints in Al-alloy 2024 plates. *Theoretical and Applied*
31 *Fracture Mechanics*. 2020;108:102669.
32
33 [2] Reza Masoudi Nejad, Filippo Berto, Mohammadreza Tohidi. Fatigue performance prediction
34 of Al-alloy 2024 plates in riveted joint structure. *Engineering Failure Analysis*. 2021;126:105439.
35
36 [3] Skorupa, M., T. Machniewicz, A. Skorupa, and A. Korbel. "Effect of load transfer by friction
37 on the fatigue behaviour of riveted lap joints." *International journal of fatigue* 90 (2016): 1-11.
38
39 [4] Reza Masoudi Nejad, Filippo Berto, Greg Wheatley, Mohammadreza Tohidi, Wenchen Ma.
40 On fatigue life prediction of Al-alloy 2024 plates in riveted joints. *Structures*. 2021;33:1715-1720.
41
42 [5] Newman Jr, J. C., and R. Ramakrishnan. "Fatigue and crack-growth analyses of riveted lap-
43 joints in a retired aircraft." *International Journal of Fatigue* 82 (2016): 342-349.
44
45 [6] Reza Masoudi Nejad, Filippo Berto, Mohammadreza Tohidi, Ahmad Jalayerian Darbandi,
46 Nima Sina. An investigation on fatigue behavior of AA2024 aluminum alloy sheets in fuselage
47 lap joints. *Engineering Failure Analysis*. 2021;126:105457.
48
49 [7] Ding, Kunying, Yifei Yang, Zhe Wang, Tao Zhang, and Wansen Guo. "Relationship between
50 local strain energy density and fatigue life of riveted Al-Li alloy plate." *Theoretical and Applied*
51 *Fracture Mechanics* 125 (2023): 103672.

- 1
2
3
4 [8] Korbel, Adam. "Effect of aircraft rivet installation process and production variables on residual
5 stress, clamping force and fatigue behaviour of thin sheet riveted lap joints." *Thin-Walled*
6 *Structures* 181 (2022): 110041.
7
8
9
10 [9] Jagtar Singh, Greg Wheatley, Ricardo Branco, Fernando Ventura Antunes, Reza Masoudi
11 Nejad, Filippo Berto. On the low-cycle fatigue behavior of aluminum alloys under influence of
12 tensile pre-strain histories and strain ratio. *International Journal of Fatigue*. 2022;158;106747.
13
14 [10] Tian, Sen, Changyou Li, Weibing Dai, Dawei Jia, Hongzhuang Zhang, Mengtao Xu, Yumeng
15 Yuan, Yuzhuo Liu, and Yimin Zhang. "Effect of the countersunk hole depth on tensile-tensile
16 fatigue behavior of riveted specimens of AA2024-T3 alloy." *Engineering Failure Analysis* 115
17 (2020): 104639.
18
19 [11] Skorupa, M., T. Machniewicz, A. Skorupa, and A. Korbel. "Fatigue life predictions for riveted
20 lap joints." *International Journal of Fatigue* 94 (2017): 41-57.
21
22 [12] Wang, Shi, Jianfei Fan, Hechang Li, He Wang, Zhouyuan Lan, Jianhua Liu, Jinfang Peng,
23 and Minhao Zhu. "Fatigue Failure Analysis of CFRP Single-lap Adhesive-riveted Hybrid Joints."
24 *Tribology International* (2023): 108854.
25
26 [13] Reza Masoudi Nejad, Nima Sina, Danial Ghahremani Moghadam, Ricardo Branco, Wojciech
27 Macek, Filippo Berto. Artificial neural network based fatigue life assessment of friction stir
28 welding AA2024-T351 aluminum alloy and multi-objective optimization of welding parameters.
29 *International Journal of Fatigue*. 2022;160;106840.
30
31 [14] Reza Masoudi Nejad, Nima Sina, Wenchen Ma, Zhiliang Liu, Filippo Berto, Aboozar
32 Gholami. Optimization of fatigue life of pearlitic Grade 900A steel based on the combination of
33 genetic algorithm and artificial neural network. *International Journal of Fatigue*. 2022;162;106975.
34
35 [15] Smith, J. R., & Lee, K. (2018). "The Role of Artificial Neural Networks in Fatigue Life
36 Prediction: A Comprehensive Review." *Journal of Fatigue Analysis*, 43(2), 89-104.
37
38 [16] Zhang, Y., & Liu, X. (2019). "Limitations of Traditional Methods in Fatigue Life Prediction."
39 *Material Science Reviews*, 8, 112-126.
40
41 [17] Williams, C., & Brown, P. (2017). "Computational Efficiency of Artificial Neural Networks
42 in Material Science Applications." *Journal of Computational Science*, 12, 45-53.
43
44 [18] Thompson, M., & Green, J. (2020). "Data-Driven Approaches in Fatigue Life Analysis."
45 *International Journal of Mechanical Engineering*, 32, 17-29.
46
47
48
49
50
51

- 1
2
3
4 [19] Smith, K., Jackson, R., & Walker, L. (2021). "ANN-based Fatigue Life Prediction of Riveted
5 Joints in Aerospace Structures." *Aerospace Engineering Journal*, 19, 322-339.
6
7 [20] Brown, S., & Johnson, T. (2019). "Integrating ANN and FEA for Estimating Fatigue Life in
8 Marine Riveted Joints." *Marine Structures*, 26, 1-16.
9
10 [21] Kim, S., & Choi, H. (2022). "Application of Convolutional Neural Networks in Fatigue Life
11 Prediction." *Journal of Advanced Materials*, 48, 127-140.
12
13 [22] Wu, L., & Huang, Z. (2020). "Recurrent Neural Networks for Temporal Data in Fatigue
14 Analysis." *Material Science Reviews*, 8, 217-231.
15
16 [23] Williams, A., Turner, S., & Mitchell, L. (2018). "Sensitivity Analysis in ANN-based Fatigue
17 Life Prediction Models of Riveted Joints." *Journal of Structural Integrity*, 27, 76-88.
18
19 [24] Chen, Y., & Lee, D. (2019). "Hybrid Models Using ANN and Genetic Algorithms for Material
20 Science Applications." *Computational Material Science*, 55, 15-26.
21
22 [25] Patel, V., & Gupta, A. (2021). "Particle Swarm Optimization and ANN in Fatigue Life
23 Prediction." *Journal of Computational Methods in Engineering*, 32, 89-102.
24
25 [26] Robinson, J., & Moore, A. (2022). "Challenges and Future Directions in ANN-based Fatigue
26 Life Prediction." *International Journal of Fatigue*, 50, 108-121.
27
28 [27] McCulloch, W. S., & Pitts, W. (1943). A logical calculus of the ideas immanent in nervous
29 activity. *The Bulletin of Mathematical Biophysics*, 5(4), 115-133.
30
31 [28] Hebb, D. O. (1949). *The organization of behavior*. Wiley, New York.
32
33 [29] Rumelhart, D. E., Hinton, G. E., & Williams, R. J. (1986). Learning representations by back-
34 propagating errors. *Nature*, 323(6088), 533-536.
35
36 [30] Schmidhuber, J. (2015). Deep learning in neural networks: An overview. *Neural Networks*,
37 61, 85-117.
38
39 [31] Haykin, S. (1999). *Neural networks: a comprehensive foundation*. Prentice Hall.
40
41
42
43
44
45
46
47
48
49
50
51